



HAL
open science

Comportement viscoélastique non linéaire des organes pleins de l'abdomen

Stéphane Nicolle, Jean-François Palierne

► **To cite this version:**

Stéphane Nicolle, Jean-François Palierne. Comportement viscoélastique non linéaire des organes pleins de l'abdomen. 22e Congrès Français de Mécanique, Aug 2017, Lyon, France. hal-04249900

HAL Id: hal-04249900

<https://hal.science/hal-04249900v1>

Submitted on 21 Nov 2024

HAL is a multi-disciplinary open access archive for the deposit and dissemination of scientific research documents, whether they are published or not. The documents may come from teaching and research institutions in France or abroad, or from public or private research centers.

L'archive ouverte pluridisciplinaire **HAL**, est destinée au dépôt et à la diffusion de documents scientifiques de niveau recherche, publiés ou non, émanant des établissements d'enseignement et de recherche français ou étrangers, des laboratoires publics ou privés.



Distributed under a Creative Commons Attribution 4.0 International License

Comportement viscoélastique non linéaire des organes pleins de l'abdomen

S. NICOLLE^{a,b,c}, J.-F. PALIERNE^{a,d}

a. Université de Lyon F-69622, Lyon, France

b. Université Claude Bernard Lyon 1, Villeurbanne ;

c. IFSTTAR, UMR-T 9406 LBMC Laboratoire de Biomécanique et Mécanique des Chocs, F-69675, Bron: stephane.nicolle@ifsttar.fr

d. Laboratoire de physique, CNRS UMR5672, Ecole Normale Supérieure de Lyon, 69007 Lyon, France : jean-francois.palierne@ens-lyon.fr

Résumé :

Cet article rassemble et compare des données obtenues au cours de précédents travaux portant sur l'identification des propriétés viscoélastiques en cisaillement du rein, du foie, de la rate et du pancréas de porc [8],[9],[10]. Le comportement linéaire et non linéaire de chaque organe a été déterminé à l'aide d'un rhéomètre en réalisant successivement deux expériences de cisaillement sur des échantillons prélevés au sein de leur parenchyme, à savoir un test harmonique aux petites déformations et un test à vitesse de déformation constante jusqu'à des déformations de l'ordre de l'unité. Sur la base des données expérimentales, un modèle viscoélastique non linéaire commun à tous les organes, formé d'une double loi de puissance en temps et en déformation, a été proposé pour décrire la réponse des organes à différentes vitesses de déformation. L'analyse des résultats montre que les quatre organes se comportent de manière identique avec, en particulier, une faible dépendance à la fréquence de leur module de cisaillement complexe et une tendance significative à raidir avec la déformation. Il apparaît toutefois que le rein est l'organe le plus rigide et le plus élastique, le pancréas est le plus mou et le plus visqueux, la rate a le régime linéaire le plus étendu tandis que le foie se raidit le plus abruptement avec la déformation.

Abstract:

This paper gathers and compares data coming from previous works [8],[9],[10] on the shear viscoelastic properties of porcine kidney, liver, spleen and pancreas. The linear and nonlinear mechanical behavior of these organs were assessed by performing in succession a harmonic test at small strain and a constant strain rate test up to strain in the order of unity. Based on these data we propose a common nonlinear viscoelastic model using a time-fractional strain-dependent kernel. These four organs behave similarly, showing in particular a weak frequency-dependence of their complex shear modulus and a significant strain-hardening. The kidney is the stiffest and the most elastic organ, the pancreas is the most compliant and the most viscous, the spleen has the most extended linear regime while the liver is most strain-hardening.

Mots clefs : Mechanical Properties, Biological Soft Tissues, Nonlinear Viscoelastic Constitutive Law

1 Introduction

Assessing and modeling the mechanical behavior of soft human tissues have been an ongoing topic for decades ([1], [2], [3]). In different human-centered research fields such as transportation safety and medicine, an exact knowledge of mechanical properties of tissues allows to determine their ‘normal’ resistance to internal and external stresses and to apprehend from a standard mechanical response the effects of biological processes such as ageing and pathologies. These researches have led to optimized prevention against the excessive accelerations sustained in road crashes and improved tools for diagnosis and therapy control.

In recent years, computational methods have been greatly involved in the progress of biomechanics. Simulations using realistic models of anatomical parts or of the whole body indeed transcend the often cumbersome and time-consuming experimentations by offering detailed information on the stress and strain experienced by the different organs. Obviously, in order to be effective, a ‘realistic’ model must implement an accurate mechanical constitutive law for the tissue.

Soft tissues can be, at first, considered as a mechanical continuum at mesoscopic scale without considering the microstructural details. Significant efforts are ongoing to improve our understanding of the deformation mechanisms (see for instance [4], [5], [6], [7]) that are particularly complex in biological soft tissues, which are highly nonlinear viscoelastic, anisotropic and heterogeneous [2]. To make the task even more complicated, they are very sensitive to the test conditions (hydration, temperature, preservation protocol...) and most of the time significantly differ from living *in situ* to dead *in vitro* situations (pressurization, vascularization, cell degradations...), in addition to inter-individual variability due to gender, age and pathology.

This paper reports on rheological data on porcine soft solid organs from previous work ([8], [9], [10]) and on the model we propose describing the common nonlinear viscoelastic behavior of these organs.

2 Materials and methods

2.1 Experiments

Rheometry is the method of choice for the current study and requires samples with a well-defined geometry.

Soft tissues were harvested from porcine organs coming from butchery (kidney, liver and spleen) or slaughterhouse (spleen and pancreas). After receipt, the organs were stored in hypothermic conditions during transportation to the laboratory. Immediately after arrival, slices of tissue with different thicknesses were prepared using a home-made double-bladed scalpel. These slices were removed from the organ parenchyma where the tissue is continuous and homogeneous. Disc-shaped 15 mm-diameter samples were then punched from the slices and conserved into a saline solution at 4°C until test.

The sample geometry was chosen to fit in the parallel-plate configuration of the used rotational rheometer (Bohlin C-VOR 150, Melvin), drawn in Fig.1. Out of the saline solution each sample was gently mopped before being glued with cyanoacrylate to the plates of the rheometer to prevent slip [11]. The sample was then surrounded with a saline solution to avoid tissue dehydration during the test at 37°C [12]. A heated cover enclosed the sample/plates system in order to reduce thermal convection and water losses.

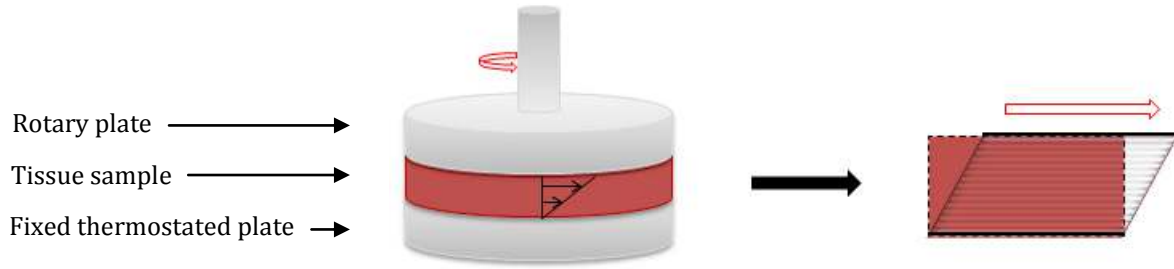


Fig. 1: Schematic of the torsional shear experiments (on the left). Locally, the sample is submitted to a simple shear deformation (on the right).

Each sample was tested in two successive ways. First, a shear oscillatory test was performed at small strain ($\sim 1\%$ strain at the edge of the sample) over a two-decade frequency range (0.1 – 10 Hz) in order to probe the linear viscoelastic properties of the tissue. The frequency was swept up and down until a steady response was obtained. The data measured during the last frequency sweep is retained. Second, immediately after the oscillatory test, the sample was subjected to one of the following constant strain rate (ramp test) 0.0151 s^{-1} , 0.133 s^{-1} or 0.6 s^{-1} up to 150% strain, in order to assess the nonlinear viscoelastic properties of the tissue. The latter experiment, being destructive, was done once for each sample and the response was used for modelling the nonlinear behavior of the tissue.

The test matrix is given in Table (1).

Table 1: Test matrix

Tissue	Test	No of samples			Strain (%)	Frequency range (Hz)	T (°C)
Kidney	Oscillatory	42			1	0.1-10	37
	Ramp	0.0151 s⁻¹ 7	0.133 s⁻¹ 8	0.6 s⁻¹ 6	0-150%		
Liver	Oscillatory	18			1	0.1-10	37
	Ramp	0.0151 s⁻¹ 5	0.133 s⁻¹ 4	0.7 s⁻¹ 4	0-150%		
Spleen	Oscillatory	38			1	0.1-10	37
	Ramp	0.0151 s⁻¹ 18	0.133 s⁻¹ 11	0.67 s⁻¹ 9	0-150%		
Pancreas	Oscillatory	33			1	0.1-10	37
	Ramp	0.0151 s⁻¹ 7	0.133 s⁻¹ 10	0.66 s⁻¹ 6	0-150%		

2.2 Constitutive law

In the K-BKZ class of models, a class of viscohyperelastic models ([21],[22]), the current shear stress $\sigma(t)$ depends on the complete past history of the shear strain $\gamma(t)$ according to the following constitutive equation:

$$\sigma(t) = \int_{-\infty}^t G(t-t', \gamma(t) - \gamma(t')) \dot{\gamma}(t') dt' \quad (1)$$

where $\dot{\gamma}(t') = d\gamma/dt'$ is the strain rate and $G(t, \gamma)$ is the strain-dependent relaxation modulus, i.e. the response of the material to a step of amplitude γ at time t after inception. We propose the following form for G :

$$G(t, \gamma) = \frac{K}{\Gamma(1-n)} t^{-n} \left\{ 1 + \left(\frac{\gamma}{\gamma_{\text{lim}}} \right)^p \right\} + \eta \delta(t) \quad (2)$$

where $\Gamma(x) = \int_0^\infty t^{x-1} e^{-t} dt$ is the Gamma function, $\delta(t)$ is the Dirac distribution, K , n and η are the material parameters which govern the linear behavior of the tissue, and γ_{lim} and p are the parameters that characterize the nonlinear behavior of the tissue.

2.3 Data Analysis

The first three parameters (K, n, η) were assessed from oscillatory tests by fitting both the storage $G'(\omega)$ and loss $G''(\omega)$ moduli of each organ by:

$$G'(\omega) = K \cos\left(\frac{n\pi}{2}\right) \omega^n \quad (3)$$

$$G''(\omega) = K \sin\left(\frac{n\pi}{2}\right) \omega^n + \eta \omega \quad (4)$$

taking $\gamma \propto \cos \omega t$, where ω is the angular frequency, in the small-strain limit $\gamma \ll \gamma_{\text{lim}}$ of Eq. (1-2). Note that $G'(\omega)$ and $G''(\omega)$ characterize the elastic and viscous properties of the tissue, respectively, their combination $G^*(\omega) = G' + iG''$ forming the so-called complex shear modulus.

After fitting the linear parameters, the last two parameters (γ_{lim}, p) were determined by fitting the torque measured at the lower constant strain rate for each organ (the intermediate strain rate was used for pancreas). The torque is given by the following equation:

$$T(t) = \frac{\pi}{2} R^3 \dot{\gamma}_R \left(\frac{K}{\Gamma(1-n)} t^{1-n} \left\{ \frac{1}{1-n} + \frac{1}{(1+p-n)(1+p/4)} \left(\frac{\dot{\gamma}_R t}{\gamma_{\text{lim}}} \right)^p \right\} + \eta \right) \quad (5)$$

that obtains by integrating the constitutive equation (1-2) over the sample boundary, the strain experienced at each point being a function of time and of the distance to the axis, where $\dot{\gamma}_R$ is the strain rate calculated at the edge of the sample for materials obeying Eq. (2) and R is the radius of the sample.

The fitting process was run for each organ using a Levenberg-Marquadt algorithm and taking into account the experimental dispersion. The adjusted R² value was calculated to measure the goodness of fit. The relevance of the model was finally assessed for each tissue by comparing its predicted response to the experimental response of the tissue at the two other strain rates.

3 Results

The results from small strain oscillatory tests are shown in Fig. (2) where the linear shear moduli of all organs are plotted against frequency. Both storage (G') and loss (G'') moduli of each tissue appear weakly frequency-dependent between 0.1 and 10 Hz and while the elastic modulus G' follows an

exact power law in frequency, the viscous modulus G'' shows an upwards deviation from an exact power law signaling the inception of a purely viscous regime at higher frequencies. The graphs show also the fits from the fractional linear model of Eq. (3-4) which remarkably matches the experimental data over the explored frequency range. The sets of linear parameters for each organ are gathered in Table (2).

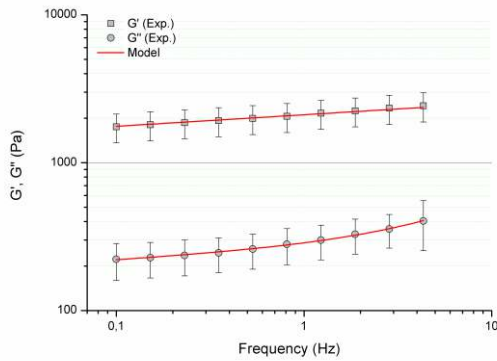
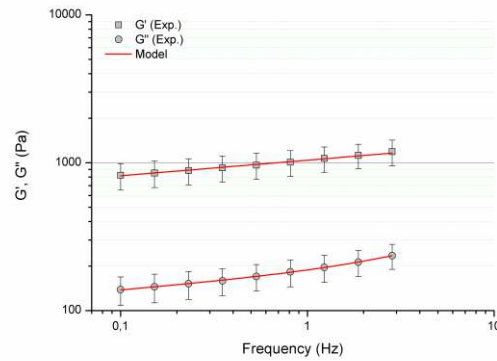
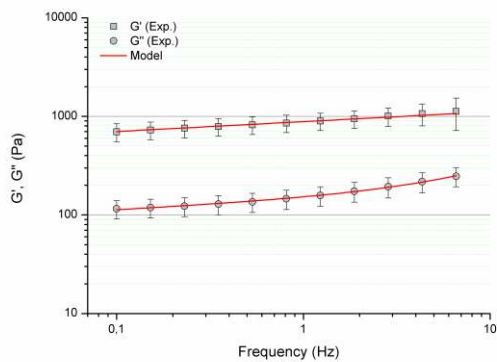
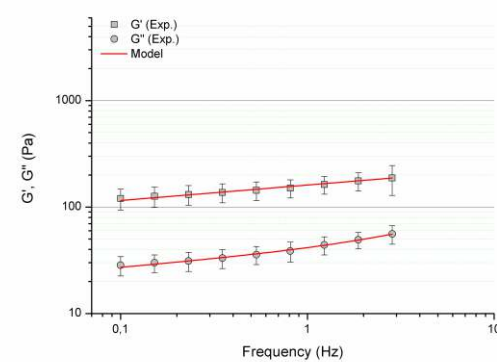
(a) Adjusted-R² = 0.9997(b) Adjusted-R² = 0.9998(c) Adjusted-R² = 0.9993(d) Adjusted-R² = 0.9980

Fig. 2: Storage and loss moduli versus frequency fitted by Eqs. (3) and (4) for (a) kidney, (b) liver, (c) spleen and (d) pancreas.

The results of the constant strain rate tests for all tissues are plotted in Fig. 3 together with the model prediction given by Eq (5). These graphs show quite clearly that each tissue experiences a strain-stiffening at all strain rates and that the proposed nonlinear model (red curves) properly captures this nonlinear feature. Two distinct straight parts are indeed visible on each response curve in a log-log representation, justifying the name of ‘bi-power law’ given to our model in [8]. The dotted lines display the torque predicted by the linear fractional model (Eq 5 for $\gamma \leq \gamma_{lim}$), evidencing that beyond γ_{lim} the torque, and then the stress, are largely underestimated if the behavior of each tissue were considered linear. To facilitate comparison between the organs all material parameters are gathered in Table (2).

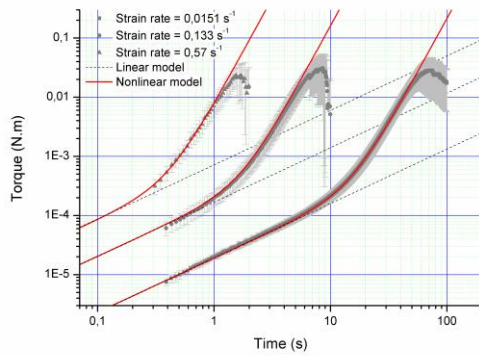
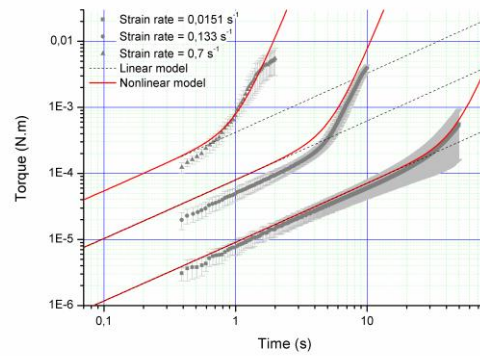
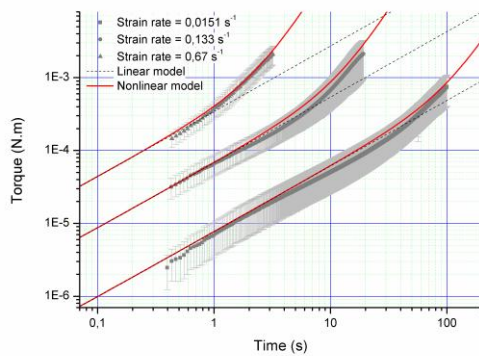
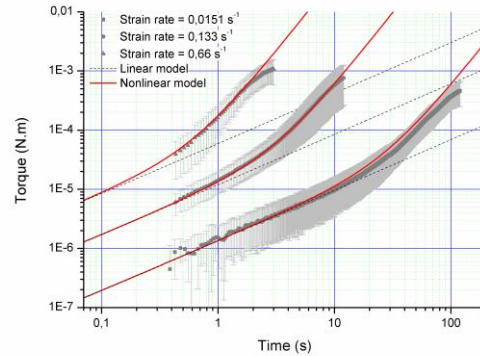
(a) Adjusted-R² = 0.9995(b) Adjusted-R² = 0.9671(c) Adjusted-R² = 0.9375(d) Adjusted-R² = 0.9990

Fig. 3: Torque according to the time at three constant strain rates fitted by our nonlinear model (Eqs. (5)) for (a) kidney, (b) liver, (c) spleen and (d) pancreas. The response of the linear model is also plotted on each graph for comparison.

Table 2: Material parameters of the porcine kidney, liver, spleen and pancreas tissues

	K (Pa.s ⁿ)	n (-)	η (Pa.s)	γ_{lim} (-)	p (-)
Kidney	1840 ± 7	0.078 ± 0.001	4.2 ± 0.2	0.1134 ± 0.0001	2.687 ± 0.003
Liver	868 ± 3	0.105 ± 0.001	2.3 ± 0.1	0.3957 ± 0.0008	3.97 ± 0.04
Spleen	742 ± 3	0.100 ± 0.001	2.0 ± 0.1	0.7700 ± 0.0100	1.77 ± 0.06
Pancreas	127 ± 1	0.145 ± 0.002	0.7 ± 0.1	0.1848 ± 0.0007	1.65 ± 0.01

4 Discussion

We aim at an analytical modeling of the nonlinear viscoelastic behavior of the human soft solid organs of the abdomen. Aware of the probable inter-species variability [13], the present paper is concerned in a first attempt with the mechanical behavior of porcine organs, available in number, less subject to individual variations (age, pathology...) and usually fresher than human ones, which are not easily available.

The main abdominal solid organs tested here (kidney, liver, spleen and pancreas) show noticeable similarities in the mechanical response of their parenchyma. First, the shear dynamic moduli of all tissues weakly depend on the frequency, as indicated by the low value of the exponent n (close to 0.1) in the time-kernel of our model. In addition the viscous behavior of all tissues showed by the loss modulus seems to initiate a transition towards a purely viscous regime at high frequencies. Second,

their deformation behavior follows a bi-power law at constant strain rate meaning that the stress sustained by these tissues follows a power law in time together with another power law in strain. In other words, the stress within the organs during a constant strain rate increases more quickly than the strain, a phenomenon named ‘strain-hardening effect’.

The phenomenological model we developed is formulated in terms of a strain-dependent fractional kernel requiring five material parameters whose meaning is given with the tissue constitution in mind. Namely, the parameter K (in Pa.s ^{n} , with $0 < n < 1$) and its companion n (dimensionless) account for the gel-like behavior of cells’ cytoskeleton and extracellular fibrous matrix. It should be noted that in the limit $n \rightarrow 0$ the model represents a Hookean solid of elastic modulus K , whereas, as $n \rightarrow 1$, it becomes a Newtonian fluid of viscosity K . Hence, intermediate values of n interpolate between viscous and elastic behavior. The parameter η making the stress directly proportional to the angular frequency ω is the purely viscous contribution of tissue inner fluid. The last two parameters γ_{lim} and p (both dimensionless) describe the strain-hardening effect due to stretching of tissue inner membranous and fibrous matrix and respectively reflect the strain linear viscoelastic limit, i.e. the strain marking the onset of the nonlinear regime, and the degree of stress-strain stiffening.

In the light of these parameters shown in Table (2), kidney appears to be the stiffest and the most elastic organ with $K = 1840 \text{ Pa.s}^{0.078}$ and $n = 0.078$, and its inner fluid to be the most viscous with $\eta = 4.2 \text{ Pa.s}$. On the opposite pancreas is the most compliant and the most viscous organ, with K almost ten times lower ($127 \text{ Pa.s}^{0.145}$) and n almost two times greater (0.145) than kidney, and with the least viscous inner fluid (0.7 Pa.s). Liver and spleen prove to be very similar in their linear viscoelastic behavior with values for K , n and η intermediate between those of kidney and pancreas. As regards strain amplitude, kidney is the organ with the least extended linear regime ($\gamma_{\text{lim}} = 11.3\%$) and the spleen has the most extended one ($\gamma_{\text{lim}} = 77\%$). Besides, the strain-hardening effect is strongest for the liver ($p = 3.97$) and weakest for the pancreas ($p = 1.65$).

These discrepancies obviously originate in the micro-structural composition and configuration of the tissues, a topic to be addressed in further works. Although the strain-stiffening of soft tissues is commonly observed in studies on different mammal soft tissues [4], [14], [15], [16], [17], a straightforward comparison of the present data with literature is not an easy task since many test conditions differ: shear/traction/compression, in vivo/ex corpus/in vitro, whole organ/tissue sample, different species, preconditioning or not, different test temperatures and measures against dehydration, different strain rates.... Some points of comparison are given in [8], [9], [10]. As regards viscoelasticity, the frequency-dependent moduli found here for the different tissues are of the same order of magnitude as those reported in the literature for kidney [18], liver [19] and pancreas [20]. The most stringent similarity in all studies is definitely the power-law frequency dependence of the moduli observed at small strain.

This last feature justifies a fractional model reproducing the linear viscoelasticity of soft tissues. The fractional kernel is supplemented with a purely viscous term to account for the fluid behavior at high frequency. A strain-dependent multiplicative factor captures the strain-hardening of the tissues.

We experienced two main experimental limitations. First, inertia effects tainted both oscillatory and strain ramp experiments, limiting the dynamic modulus measurements to frequencies below 8 Hz and precluding the torque readings at time shorter than 400 ms respectively. Second, failure of the sample gluing caused an abrupt drop of the torque at large deformation as can be seen for the kidney tissue on Fig. (3). In consequence, the shear tests performed in the current conditions are unable to probe the rupture mechanics of tissues.

5 Conclusions

This paper reports on a comparative synthesis of shear mechanical properties of porcine kidney, liver, spleen and pancreas studied in previous works [8], [9], [10] using a rotational rheometer. Oscillatory and strain ramp experiments revealed that the tissues display a gel-like behavior with weakly frequency-dependent shear moduli and a significant strain-stiffening. The five-parameter model we developed for predicting the nonlinear shear response of tissues shows a remarkable agreement with the experimental data. Using the latter in a comparative analysis revealed that the kidney is the stiffest and the most elastic organ, the pancreas is the most compliant and the most viscous, the spleen has the most extended linear regime whilst the liver shows the strongest strain-hardening effect.

Références

- [1] H. Yamada, Strength of biological materials, The Williams & Wilkins Company, Baltimore, USA (1970)
- [2] Y.C. Fung, Biomechanics: Mechanical properties of living tissues, 2nd Edition, New-York (1993)
- [3] G.A. Holzapfel, Similarities between soft biological tissues and rubberlike materials, In: P.-E. Austrell and L. Keri (eds.), 'Constitutive models for rubber IV', A.A Balkema Publishers: Leiden (2005) 607-617
- [4] M. Farshad, M. Barbezat, P. Flüeler, F. Schmidlin, P. Graber, P. Niederer, Material characterization of the pig kidney in relation with biomechanical analysis of renal trauma, *Journal of Biomechanics* 32 (1999) 417-425
- [5] A. Tamura, K. Omori, K. Miki, K.H. Yang, A. King, Mechanical characterization of porcine abdominal organs, *Stapp Car Crash Journal* 46 (2002) 55-69
- [6] M.Z. Kiss, T. Varghese, T.J. Hall, Viscoelastic characterization of in vitro canine tissue, *Physics in Medicine and Biology* 49 (2004) 4207-4218
- [7] J. Rosen, J.D. Brown, S. De, M. Sinanan, B. Hannaford, Biomechanical properties of abdominal organs in vivo and post-mortem under compression loads, *Journal of Biomechanical Engineering* 130 (2008) 021020.1-021020.17
- [8] S. Nicolle, P. Vezin, J.-F. Paliérne, A strain-hardening bi-power law for the nonlinear behavior of soft tissues, *Journal of Biomechanics* 43 (2010) 927-932
- [9] S. Nicolle, L. Noguier, J.-F. Paliérne, Shear mechanical properties of the spleen: Experiment and analytical modelling, *Journal of the Mechanical Behavior of Biomedical Materials* 9 (2012) 130-136
- [10] S. Nicolle, L. Noguier, J.-F. Paliérne, Shear mechanical properties of the pancreas: Experiment and analytical modelling, *Journal of the Mechanical Behavior of Biomedical Materials* 26 (2013) 90-97
- [11] S. Nicolle, J.-F. Paliérne, On the efficiency of attachment methods of biological soft tissues in shear experiments, *Journal of the Mechanical Behavior of Biomedical Materials* 14 (2012) 158-162
- [12] S. Nicolle, J.-F. Paliérne, Dehydration effect on the mechanical behavior of biological soft tissues: Observations on kidney tissues, *Journal of the Mechanical Behavior of Biomedical Materials* 3 (2010) 630-635
- [13] A.R. Kemper, A.C. Santago, J.D. Stitzel, J.L. Sparks, S.M. Duma, Biomechanical response of human spleen in tensile loading, *Journal of Biomechanics* 45 (2012) 348-355
- [14] J.W. Melvin, R.L. Stalnaker, V.L. Roberts, M.L. Trollope Proceedings of the 17th Stapp car Crash Conference (1973) 115-126

- [15] J.L. Sparks, R.B. Dupaix Constitutive modelling of rate-dependent stress-strain behavior of human liver in blunt impact loading, *Annals of Biomedical Engineering* 36 (2008) 1883-1892
- [16] H. Saraf, K.T. Ramesh, A.M. Lennon, A.C. Merkle, J.C. Roberts, Measurement of dynamic bulk and shear response of soft human tissues, *Experimental Mechanics* 47 (2007) 439-449
- [17] N.H. Nguyen, M.T. Duong, T.N. Tran, P.T. Pham, O. Grottko, R. Tolba, M. Staat, Influence of freeze-thaw cycle on the stress-stretch curves of tissues of porcine abdominal organs, *Journal of Biomechanics* 45 (2012) 2382-2386
- [18] S. Nasser, L.E. Bilston, N. Phan-Thien, Viscoelastic properties of pig kidney in shear, experimental results and modelling, *Rheologica acta* 41 (2002) 180-192
- [19] C. Wex, A. Stoll, M. Fröhlich, S. Arndt, H. Lippert, How preservation time changes the linear viscoelastic properties of porcine liver, *Biorheology* 50 (2013) 115-131
- [20] C. Wex, M. Fröhlich, K. Brandstädter, C. Bruns, A. Stoll, Experimental analysis of the mechanical behavior of the viscoelastic porcine pancreas and preliminary case study on the human pancreas, *Journal of the Mechanical Behavior of Biomedical Materials* 41 (2015) 199-207
- [21] B. Bernstein, E.A. Kearsley, L.J. Zapas, A study of stress relaxation with finite strain, *Transactions of the Society of Rheology* 7 (1963) 391-410
- [22] E. Mitsoulis, 50 year of the K-BKZ constitutive relation for polymers, *International Scholarly Research Notices Polymer Sciences* 2013 (2013), Article ID 952379